Rev.Adv.Mater.Sci. 10 (2005) 403-408

CRACKING IN Si-BASED ANODES FOR Li-ION BATTERIES

K.E. Aifantis[1], J.P. Dempsey[2] and S.A. Hackney[3]

[1]Dept of Applied Physics, University of Groningen, The Netherlands
[2]Dept of Civil and Environmental Engineering, Clarkson University, USA
[3]Dept of Materials Science and Engineering, Michigan Technological University, USA

Received: June 25, 2005

Abstract. In attempts to increase the anode capacity of rechargeable Li-ion batteries, composite materials with micro- and nano-scale domains of Li active material surrounded by Li inactive material are being investigated. Materials such as Si, Al and Sn that provide capacities between 900 and 4000 mAh g^{-1} during the formation of Li-alloys can be used as the active sites, while inert ceramics or glasses can be as the inactive matrix. During Li insertion the volume of the active sites expands over 100% at maximum capacity. As a result large internal stresses are produced, which lead to a loss of mechanical integrity at the active site/matrix interface and eventually cracking of the electrode. Therefore, before these types of composite material systems are used commercially it is of great importance to model their mechanical response. The present study applies a previously developed formulation to predict stable crack growth in anodes which are comprised of spherical Si nanospheres embedded in a soda glass matrix.

1. INTRODUCTION

Due to the large volumetric and gravimetric energy densities exhibited by Li battery chemistries, rechargeable Li-ion batteries are the main energy sources used in electronic devices such as laptop computers and cell phones. These types of battery chemistries have also seen use in biomedical, implantable devices. Initially, the Lithium metal was used as the negative electrode in Li-ion batteries, but due to safety issues graphitic anodes have been used commercially since the 1970's. Graphite, however, has a very low Li atomic density at full Li capacity in the carbon intercalation compound (LiC_6), resulting in a relatively low volumetric Li capacity. This is an important aspect in choosing the electrode materials because the total amount of Li-ions that can be taken up by the electrode material corresponds to the total time integration of the battery current. Therefore extensive research is being performed for the development of alternative anode materials that would give a higher energy density for the Li-ion battery systems. Some experimental research indicates that promising candidates for next generation Li-ion negative electrodes are engineered materials exhibiting a micro- or nano-scale composite structure. These nano-composites are comprised of materials capable of forming Li rich compounds (active materials) surrounded by a matrix of materials that are inert with respect to Li (inactive materials). Both Si and Sn are very good candidates for the active material in the composite structures as

Corresponding author: K.E. Aifantis, e-mail: k.aifantis@damtp.cam.ac.uk

they have a very high Li intercalation density per host atom, forming the compounds $Li_{4.4}Si$ and $Li_{4.4}Sn$. In terms of the total time integrated battery current per mass, these compounds have capacities of 4000 and 900 mAh g^{-1}, respectively [1], whereas graphitic carbon gives a much lower Li capacity of 372 mAh g^{-1} [2]. The drawback, however, is that during maximum Li insertion Si suffers a 310% volume increase [1]; in fact all metals that can act as active sites such as Sn, Bi, Sb, Al exhibit over a 100% volume increase after Li alloy formation. As a result significant internal stresses are produced and during the initial electrochemical cycles loss of mechanical integrity takes place at the active site/matrix interface; this leads to a loss of electrical integrity and fracture of the electrode [1].

A first attempt to model this loss of mechanical integrity in battery electrodes was done by treating the damage zone at the active site/matrix interface as consisting of multiple radial cracks [3] emanating into the glass matrix from Sn particles, which acted as the active sites. Various geometrical configurations that are currently under experimental consideration were considered, i.e. thin film electrodes, fibre like active site inclusions and nanospherical Sn inclusions, along with possible variations in elastic boundary conditions that might be possible in practical situations. In the present study this formulation will be applied to Si-based anodes, since they have favourable electrochemical properties (capacity and Li intercalation). The Si active sites will be taken to be spherical with a nanometre diameter, according to experimental observation, and will be surrounded by a soda glass matrix.

2. ANODE CONFIGURATION

The configuration of the problem at hand is shown in Fig. 1. It should be noted here that the crumbling effect at the active site/matrix interface is significantly reduced for active sites that have nanometre dimensions, such as spherical nanocrystalline Si particles with a 10 nm radius [2]. Additionally, this miniaturization is very effective from an electrochemical point of view since bulk Si reacts with Li at very large temperatures (400K), whereas nanocrystalline Si can form Li alloys at room temperature [4]. It should also be noted that the capacity of bulk Si is significantly reduced after a few cycles [5], whereas at the nanorange it is closer to its theoretical value; i.e. 3000 mAh·g^{-1} have been achieved for 40 nm thin films, after 25 cycles [6]. Based on this experimental background the anode is taken to be comprised

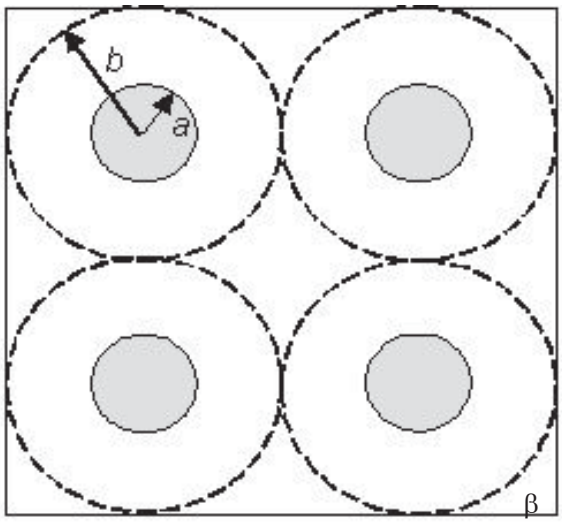

Fig. 1. Idealized geometry of the electrode: Li-insertion particles (shaded) embedded in a glass (blank) matrix. A unit cell is defined by a circle of radius *b* surrounding a circular particle of radius *a*.

of Si nanospheres embedded in an inert, with respect to Li, matrix. Although thorough experimental studies concerning the selection of the most appropriate matrix do not exist, it is assumed here that the matrix is soda glass, which is a direct extension of [3] and [7].

As was mentioned in the introduction after the first few electrochemical cycles crumbling occurs at the Si/matrix interface. Since the matrix is more brittle from the Si it is assumed that the soda glass crumbles and forms a damage zone, as shown in Fig. 2. Since this region is severely damaged it is believed to support only radial stresses, and can therefore be approximated by a number of radial cracks with length ρ-*a*. Furthermore, it should be noted that in Fig. 2, a and b are the radii of the Si and soda glass, while Δ is the radial displacement to which the Si would expand to if it were not surrounded by the matrix.

3. CRACK PROPAGATION

3.1. Stress and displacement expressions in Si / damage zone / uncracked glass

This section is a summary of the wok presented in [3]. Since the state of maximum Li insertion is being examined the stress that the Li-ions exert inside the Si is constant and therefore the pressure

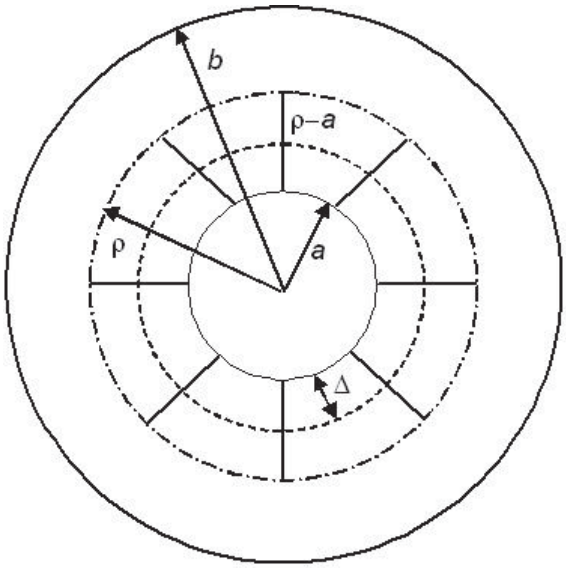

Fig. 2. Radial cracking for assumed configuration.

that the active site exerts onto the matrix is equal to *p*. Similarly the pressure that is exerted onto the unit cell under examination by a neighbouring cell is constant and equal to *q*. This implies the conditions

$$\sigma_r(a) = -p, \sigma_r(b) = -q\,. \tag{1}$$

Since conditions of spherical symmetry are present the stress and displacement expressions in the Si can be written as

$$\sigma_r \equiv \sigma_{rr} = \sigma_{\theta\theta} = \sigma_{\Phi\Phi} = 2\frac{1+\nu_s}{1-2\nu_s}D_s;$$
$$u_r = \frac{2(1+\nu_s)r}{E_s}D_s; \tag{2}$$

where it is noted that in the first expression of Eq. (2) there is no variation the *r*-direction since upon maximum Li insertion the stress is uniform inside the Si.

Consideration of Eqs. (1) and (2) allows the displacement inside the Si to be expressed as

$$u_r = -\frac{(1-2\nu_s)rp}{E_s}. \tag{3}$$

Now we can develop a displacement condition at the active site/matrix interface as follows. If the Si was not surrounded by soda glass, upon maximum Li insertion it would attain a radius of $r = a + \Delta$. The surrounding matrix, which is present under the given confined configuration, opposes the aforementioned free expansion by pushing back the active site by a distance δ; therefore the final radius of the Si, under the present case, is $r = a + \Delta - \delta$, and the total displacement of the outer surface of the Si particle at $r = a + \Delta$ is $u_r = -\delta$. Alternatively we can write

$$u_r(a+\Delta) = -\delta = -\frac{(1-2\nu_s)(r+a)p}{E_s}. \tag{4}$$

Similarly the displacement at the Si/matrix interface can be formulated by considering the initial inner radius of the glass annulus, wich is $r = a$ and that which it attains after maximum Li insertion which is $r = a + \Delta - \delta$ (according to the previous reasoning). Therefore at the Si/glass interface ($r = a$) $u_r = \Delta$-δ. Combining this boundary condition with Eq. (4) gives

$$u_r(a) = \Delta - \delta = \Delta - \frac{(1-2\nu_s)(r+a)p}{E_s}. \tag{5}$$

Now the stress and displacement expressions inside the next region of Fig. 2, which is the damage zone, need to be developed. As was already mentioned this region is severely damaged such that it can support only radial stresses, hence the stress equibrium relation gives

$$\frac{d\sigma_r}{dr} + \frac{2\sigma_r}{r} = 0 \Rightarrow \sigma_{rr}(r) = \frac{k}{r^2}, \text{ for } a \le r \le \rho. \tag{6}$$

Furthermore the displacement expression is deduced as

$$\sigma_{rr}(r) = E_g\frac{du_r}{dr} \Rightarrow \frac{du_r}{dr} = -\frac{pa^2}{E_g r^2} \Rightarrow$$
$$u_r(r) = \frac{pa^2}{E_g r} + u^*. \tag{7}$$

Combining Eq. (6) with the first expression in Eq. (1) implies that the constant of integration *k* is k = -pa^2; while *u** is found by setting the displacement right in front of the crack tip $u_+(\rho)$ equal to $u_\gamma(\rho)$, i.e.

$$u_+(\rho) = u_r(\rho) = \frac{pa^2}{E_g\rho} + u^* \Rightarrow$$
$$u^* = u_+(\rho) - \frac{pa^2}{E_g\rho}. \tag{8}$$

Insertion now of Eq. (8) into Eq. (7) gives the displacement expression inside the damage zone as

$$u_r(r) = \frac{pa^2}{E_g}\left(\frac{1}{r} - \frac{1}{\rho}\right) + u_+(\rho) \text{ for } a \le r \le \rho . \quad (9)$$

Finally, the displacement expression inside the uncracked matrix, i.e. a hollow sphere which experiences an internal pressure (by the Si site) and an external pressure (by the neighboring unit cell), is given in [8] as

$$u_+(r) = \frac{r(1+\nu_g)}{E_g}\left\{ p_* \frac{\frac{b^3}{2r^3} + (1-2\nu_g)(1+\nu_g)}{\frac{b^3}{\rho^3} - 1} - q\frac{\frac{\rho^3}{2r^3} + (1-2\nu_g)(1+\nu_g)}{1 - \frac{\rho^3}{b^3}}\right\}, \text{ for } \rho \le r \le b . \quad (10)$$

The internal pressure p_* is the pressure exerted at $r = \rho$, and is found through Eq. (6) to be $p_* = (pa^2)/\rho^2$.

It follows that by letting $r = \rho$ in Eq. (10) an analytical expression can be obtained for $u_+(\rho)$, which can then be substituted in Eq. (9) for the development of a second boundary condition at the Si/glass interface as

$$u(a) = \frac{pa^2}{E_g}\left\{\frac{1}{a} - \frac{2(1-\nu_g)}{\rho} + \frac{3(1-\nu_g)(b^3 - Sbp^2)}{2\rho(b^3 - \rho^3)}\right\}, \quad (11)$$

where, $S = qb^2/(pa^2)$. Finally, the displacement at the outer glass boundary ($r=b$) is found by direct substitution in Eq. (11)

$$u(b) = \frac{pa^2}{2bE_g}\left\{\frac{3(1-\nu_g)(b^2\rho - Sb^3)}{b^3 - \rho^3} + S(1+\nu_g)\right\}. \quad (12)$$

3.2. Stability index formulation

For the present configuration, $\sigma_{\theta\theta}$ may be thought of as being the opening tensile stress responsible for crack stability and growth. It has been solved in [9] that for a radial configuration, such as that in Fig. 2, the hoop stress is given as

$$\sigma_{\theta\theta}(\rho^+) = \frac{pa^2}{b^2}\left[\frac{1 - 3S\left(\frac{\rho}{b}\right)^2 + 2\left(\frac{\rho}{b}\right)^3}{2\left(\frac{\rho}{b}\right)^2\left(1 - \left(\frac{\rho}{b}\right)^3\right)}\right], \quad (13)$$

while the corresponding energy release rate for such a system is

$$G(\rho) = \frac{2(1-\nu_g)\rho\sigma^2_{\theta\theta}(\rho^+)}{nE_g}. \quad (14)$$

Finally, the stability index can defined according to [10] as

$$\kappa = \frac{b}{G}\frac{dG}{d\rho}. \quad (15)$$

In order to apply the above formulation to Si-based anodes three different outer boundary conditions will be considered.

Case 1: Clamped outer boundary

The first case, which is considered, corresponds to the common 'manufacturing consistent' configuration according to which the battery system is tightly constrained by the outer casing and, therefore, the displacement at the glass/glass interface is zero. Therefore, $u(b)=0$ and by setting Eq. (12) equal to zero S is found to be

$$S = \frac{3(1-\nu_g)b^2\rho}{2(1-2\nu_g)b^3 + (1+\nu_g)\rho^3}. \quad (16)$$

Inserting Eq. (16) in Eq. (11) and then setting the resulting expression equal to Eq. (5), gives the internal pressure, p_1, which can in turn be substituted in Eq. (14) to give

$$G_1 = \frac{2(1-\nu_g)a^4 p_1^2}{nE_g\rho^3}\left[\frac{(1-2\nu_g)b^3 - (1+\nu_g)\rho^3}{2(1-2\nu_g)b^3 + (1+\nu_g)\rho^3}\right]^2, \quad (17)$$

where

$$p_1 = \Delta\left\{\frac{a^2}{\rho E_g}\left[\frac{\rho}{a} - 2(1-\nu_g) + \frac{3(1-\nu_g)(1-2\nu_g)b^3}{2(1-2\nu_g)b^3 + (1+\nu_g)\rho^3}\right] + \frac{(a+\Delta)}{\Gamma^{sph}}\right\}^{-1}. \quad (18)$$

It should be noted that in Eq. (18) as well as in the following relations $\Gamma^{sph}=E_s/(1-2\nu_s)$.

Case 2: Traction free outer boundary

The second configuration was formulated by considering the 'natural' condition, according to which the pressure that is induced on the glass by the active site fades with increasing distance and hence the outer pressure (at the glass/glass interface) is zero. Therefore, q=0 (which implies that S=0), and thus, Eqs. (11) and (5) can be used as before to determine the internal pressure, for this case, p_2. Then, by using Eqs. (13) and (14) the energy release rate, G_2, is readily calculated as

$$G_2 = \frac{(1-\nu_g)a^4 p_2^2}{2nE_g\rho^3}\left[\frac{b^3+2\rho^3}{b^3-\rho^3}\right]^2, \qquad (19)$$

where

$$p_2 = \Delta\left\{\frac{a^2}{\rho E_g}\left[\frac{\rho}{a}-2(1-\nu_g)+\frac{3(1-\nu_g)b^3}{2(b^3-\rho^3)}\right]+\frac{(a+\Delta)}{\Gamma^{sph}}\right\}^{-1}. \qquad (20)$$

Case 3: Self-equilibrating loading

The final case to be considered is that of 'self-equilibrated loading', according to which the force (qb^2) that is exerted on the glass annulus by the surrounding unit cell is equal to that exerted onto it by the Li insertion site (pa^2). Therefore S=1, and solving for the internal pressure as before, the energy release rate, G_3 , for this case is found to be

$$G_2 = \frac{(1-\nu_g)a^4 p_3^2}{2nE_g\rho^3}\left[\frac{(b+2\rho)(b-\rho)}{b^2+bp+\rho^2}\right]^2, \qquad (21)$$

where

$$p_3 = \Delta\left\{\frac{a^2}{\rho E_g}\left[\frac{\rho}{a}-\frac{(1-\nu_g)}{2}-\frac{3(1-\nu_g)\rho^2}{2(b^2+bp+\rho^2)}\right]+\frac{(a+\Delta)}{\Gamma^{sph}}\right\}^{-1}. \qquad (22)$$

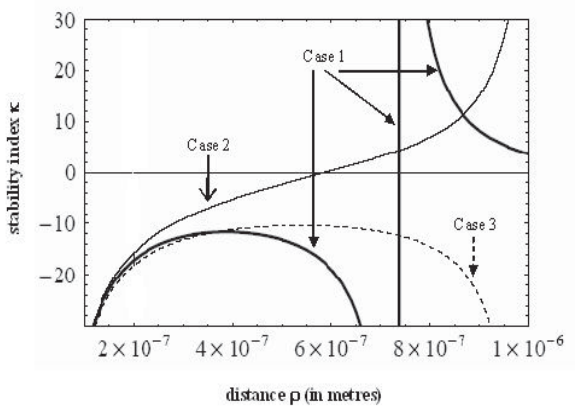

Fig. 3. Stable crack growth in negative electrode with spherical Si active sites embedded in a soda glass matrix.

4. DISCUSSION

Now the stability index, κ, can be computed for each case, via Eq. (15), by letting the radii (a and b) and the material parameters (E_s, E_g, ν_s, ν_g) be (100 nm and 1000 nm) and (41 GPa, 75 GPa, 0.33, 0.25) [10] respectively. As was mentioned in the introduction the volume expansion of Si is 310% [1, 11]; this implies that its final radius upon maximum Li insertion will be 310nm, and therefore $\Delta=r_{\text{after expansion}}-r_{\text{before expansion}}$=310-100=210 nm. (It should be noted that n need not be quantified since κ is independent of the number of radial cracks that form.) Now a stability diagram can be constructed by plotting κ with respect to ρ (Fig. 3). These diagrams suggest that stable crack growth (i.e. slow crack propagation velocities) occurs for negative values of the stability index. In fact the more negative κ the more stable the crack propagation since the energy difference is smaller. Once the x-axis is crossed (i.e. κ becomes positive) the crack velocities increase and catastrophic failure is approached more rapidly, hence growth becomes unstable; it follows that the turning point from stable to unstable growth indicates the critical stable crack length. It should be noted that the asymptote obtained for the manufacturing consistent case indicates that as the length ρ approaches the asymptote the cracks will be closed shut. Case 2 therefore is the most favorable configuration according to this analysis since crack growth not only is stable but once the cracks reach a critical length they will be pinched shut. Case 1 on the other hand is inherently unstable; while Case 3 allows for stable crack growth until the outer boundary of the unit cell is reached. It should be noted that it has been observed experimentally that cracks which initiate at the active site surface may close shut after a few electrochemical cycles [1]. These

results are encouraging, but a direct comparison with the present formulation cannot be made yet, since they were obtained for thin film electrodes deposited on substrates. It should be noted that the stability plot for Si active sites obtained herein is almost identical to the corresponding plot obtained in [3] for Sn active sites. This implies that the elastic properties of the matrix, not the active site, play a detrimental role in the value of the stable critical crack length. It follows that application of the aforementioned formulation to electrodes in which Sn or Si act as the active sites, while various ceramics/glasses act as the inert matrix, can provide important insight concerning the most appropriate matrix material for these alternative Li-ion battery anodes. Such a study is under progress.

ACKNOWLEDGEMENTS

K.E.A. is grateful to the US National Science Foundation for its support through its Graduate Research Fellowship Program. J.P.D. would like to acknowledge the support of the US Army (by Grant DAAD 19-00-1-0479) and the National Science Foundation (by the OPP Grant 0338226).

REFERENCES

[1] L. Y. Beaulieu, K. W. Eberman, R. L. Turner, L. J. Krause and J. R. Dahn // *Electrochem. Solid-State Lett.* **4(9)** (2001) A137.
[2] J. Graetz, C. C. Ahn, R. Yazami and B. Fultz // *Electrochem. Solid-State Lett* **6 (9)** (2003) A194.
[3] K.E. Aifantis and J.P. Dempsey // *J. Power Sources* **143** (2005) 203.
[4] B. Gao, S. Sinha, L. Fleming and O. Zhou // *Adv. Matls* (2005), in print.
[5] H. Li, X. Huang, L. Chen, Z. Wu and Y. Liang // *Electrochem. Solid-State Lett* **2** (1999) 547.
[6] T. Takamura, S. Ohara, J. Suzuki and K. Sekine, *The 11th International Meeting on Lithium Batteries* (Monterey, CA, June 23-28, 2002), Abstract 257.
[7] K.E. Aifantis and S.A. Hackney // *J. Mech. Behav. Matls* **14** (2003) 413.
[8] H.M. Westergaard, *Theory of Elasticity and Plasticity* (Harvard University Press, 1953).
[9] J.P. Dempsey, L.I. Slepyan and I.I. Shekhtman // *Int. J. Fract.* **73** (1995) 223.
[10] J.P. Dempsey, A.C Palmer and D.S Sodhi // *Eng. Fract. Mech.* **68** (2001) 1961.
[11] T. Moon, C. Kim and B. Park // *J. Power Sources* (2005), in press.